Submicron aerosol composition at Trinidad Head, California, during ITCT 2K2: Its relationship with gas phase volatile organic carbon and assessment of instrument performance

James D. Allan,[1] Keith N. Bower,[1] Hugh Coe,[1] Hacene Boudries,[2] John T. Jayne,[2] Manjula R. Canagaratna,[2] Dylan B. Millet,[3] Allen H. Goldstein,[3] Patricia K. Quinn,[4] Rodney J. Weber,[5] and Douglas R. Worsnop[2]

Received 2 October 2003; revised 21 January 2004; accepted 15 March 2004; published 7 July 2004.

[1] Two Aerodyne aerosol mass spectrometers (AMSs) were deployed at Trinidad Head on the north Californian coast during the National Oceanographic and Atmospheric Administration Intercontinental Transport and Chemical Transformation 2002 (ITCT 2K2) experiment, to study the physiochemical properties of submicron aerosol particles within the Pacific marine boundary layer. One AMS was modified to allow the study of sea salt-based particles, while the other used a temperature cycling system on its inlet. The reported loadings increased by a factor of 2 when the temperature approached the dew point, which is due to the inlet performance and has implications for other AMS experiments and applications. The processed data were compared with those of a particle into liquid sampler-ion chromatograph and showed that the ammonium, sulfate and organic fractions of the particles were consistently found within a single, normally acidic, accumulation mode at around 300–400 nm. However, when influenced by land-based sources, vehicle emissions and increased ammonium loadings were seen. The concentrations of nitrate in the accumulation mode were low, but it was also found within sea salt particles in the coarse mode and can be linked to the displacement of chloride. The organic fraction showed a high degree of chemical ageing and evidence of nitrogen-bearing organics was also observed. The particulate organic data were compared to the volatile organic carbon data derived from an in-situ gas chromatograph-mass spectrometer-flame ionization detector and relationships were found between the gas and particle phase chemicals in both the overall concentrations and the levels of oxidation. *INDEX TERMS:* 0305 Atmospheric Composition and Structure: Aerosols and particles (0345, 4801); 0365 Atmospheric Composition and Structure: Troposphere—composition and chemistry; 0368 Atmospheric Composition and Structure: Troposphere—constituent transport and chemistry; 0394 Atmospheric Composition and Structure: Instruments and techniques; 9355 Information Related to Geographic Region: Pacific Ocean; *KEYWORDS:* marine boundary layer, aerosol mass spectrometry, particles

Citation: Allan, J., et al. (2004), Submicron aerosol composition at Trinidad Head, California, during ITCT 2K2: Its relationship with gas phase volatile organic carbon and assessment of instrument performance, *J. Geophys. Res.*, *109*, D23S24, doi:10.1029/2003JD004208.

1. Introduction

[2] Aerosols are recognized as an important, if relatively poorly understood, component of the earth's atmosphere. They are known to be a significant factor when considering the planetary albedo, as they can absorb and scatter light (the direct radiative effect) and can alter the properties of clouds by affecting their lifetimes and optical properties (the indirect radiative effect). Although much research is performed on continental aerosols, as these contain the highest concentration of particles of anthropogenic origin, aerosols within the marine boundary layer (MBL) are of no less importance. The oceans are known to be a very large source of sulfate-based particles, created indirectly through the emission of dimethyl sulfide (DMS) by phytoplankton. As sulfate particles readily form cloud condensation nuclei (CCN), they play an important role in theoretical predictions of cloud activity and climate properties [*Ayers et al.*, 1991; *Charlson et al.*, 1987]. The ocean is also a source of coarse mode particles, principally made of sea salt, formed by bursting bubbles and wave action.

[1]Department of Physics, University of Manchester Institute of Science and Technology, Manchester, UK.
[2]Aerodyne Research Inc., Billerica, Massachusetts, USA.
[3]Environmental Science, Policy and Management, University of California at Berkeley, Berkeley, California, USA.
[4]NOAA Pacific Marine Environmental Laboratory, Seattle, Washington, USA.
[5]School of Earth and Atmospheric Sciences, Georgia Institute of Technology, Atlanta, Georgia, USA.

0148-0227/04/2003JD004208$09.00

[3] As the prevailing winds in western North America carry air from the west, the background atmosphere in this region is impacted by the detailed composition of the Pacific MBL. Thus the characterization of the Pacific MBL, particularly with respect the particulate matter (PM), is one of the primary goals of the National Oceanographic and Atmospheric Administration (NOAA) Intercontinental Transport and Chemical Transformation 2002 (ITCT 2K2) experiment. Sources of the PM arriving at the Pacific coast may include emissions from the ocean, aged PM from sources in East Asia, mixing from the free troposphere, pollution from shipping routes and ''local'' emissions from the continental North America.

[4] Two Aerodyne Aerosol Mass Spectrometers (AMSs) [*Jayne et al.*, 2000] were deployed at the Trinidad Head supersite on the north California coast during ITCT 2K2 in April and May 2002. The deployment was jointly operated by the University of Manchester Institute of Science and Technology (UMIST) and Aerodyne Research Incorporated (ARI). The purpose of the measurements was to characterize submicron particle size and chemistry in the MBL as it arrived at the Pacific coast with a high time resolution. The AMS works by focusing sampled particles into a tightly collimated beam using an aerodynamic lens [*Liu et al.*, 1995a, 1995b], skimming off the majority of the gas phase material and impacting them on a heated tungsten surface (called the vaporizer) under ultra-high vacuum. The resultant vapors are analyzed using quadrupole mass spectrometry. This system can quantitatively study the nature and total mass concentrations of the nonrefractory components of submicron aerosol particles (The term ''nonrefractory'' is operationally defined as those chemicals that vaporize in less than a second on the heated surface). It is also capable of sizing particles aerodynamically. One advantage of the instrument is that it is capable of delivering size-resolved data with a time and diameter resolution many times higher than can be achieved with bulk samplers such as cascade impactors. Additionally, the AMS is also able to deliver data on the chemical nature of the organic matter (OM) fraction of the particles. While it cannot identify specific compounds, it is able to deliver information on the types of organics present. The UMIST instrument was also modified from its standard configuration to allow the study of less volatile sea salt particles.

2. Experimental

[5] The site at Trinidad Head (41.054°N, 124.151°W, 107 m elevation) was on a coastal cliff top in northern California. The two AMSs sampled ambient air through a 2.5 μm cutoff cyclone (URG-200-30EN, URG, USA), positioned 15 meters above ground level on a scaffold tower.

[6] The first instrument, referred to as the Aerodyne Research Inc. (ARI) instrument, was operated under the standard configuration and protocol for ambient aerosol sampling [*Jimenez et al.*, 2003a], except for using a temperature control system on its inlet. Water was recirculated around the assembly containing the critical orifice at the instrument's inlet and the tubing leading up to the instrument. The water was fed from a refrigerated bath, maintained at 2°C, passing over an AC heating coil. The temperatures of the inlet and recirculating water were measured using thermocouples (OMEGA Engineering Inc., CT, USA), interfaced to the logging computer. The power to the heating coil was switched on and off digitally on a forty minute cycle, which ramped the inlet temperature up and down. By adjusting the water flow rate and the voltage applied to the heating coil, the magnitude and the ramp rate of the temperature cycle could be adjusted. Generally, the low extreme of the cycle was matched to the ambient dew point and the high extreme to approximately 20°C above the ambient dew point. The dew point temperature (t_d) data were calculated using temperature (t) and relative humidity (RH) data from a HMP45C probe (Campbell Scientific Inc.) located on the tower.

[7] The second instrument, hereafter referred to as the UMIST AMS, was modified to be able to detect sea salt particles. In the standard configuration, it is possible to run the vaporizer at a high enough temperature to vaporize sodium chloride particles, but at these temperatures a significant proportion of atoms such as sodium and potassium become ionized thermally rather than by electron impact. This ''surface ionization'' is very undesirable because it produces positive ions in very large numbers and does not easily yield quantitative data. Several laboratory experiments were conducted at ARI to optimize the AMS in order to measure the sea salt aerosol composition present in ambient aerosol. The modification of the AMS consists of physically moving the vaporizer 3 mm away from the quadrupole detection region, adding a negative bias voltage until the background sodium signal becomes very low and operating it at a temperature of about 850°C. In this configuration, any positively charged sodium and potassium ions produced by the vaporizer are unable to overcome the potential difference between the surface of the vaporizer and the ionization region, and so only the neutral atoms are able to reach the detection region. These are subsequently ionized by electron impact and are detected. The tradeoff was that the instrument's overall sensitivity was reduced, due to both the increased distance between the heated surface and the detection region and the fact that the vaporized molecules, having a higher thermal velocity, spent less time in the detection region compared with the standard configuration. While this reduction in sensitivity was accounted for by the calibration protocol, it in turn affected the signal-to-noise ratios of the data. Also, the high vaporizer temperature meant that organic species were subject to additional thermal fragmentation, making the mass spectral identification of the types of organic chemicals in the particles more difficult.

[8] An automated in-situ gas chromatograph - mass spectrometer - flame ionization detector (GC-MS-FID) system was deployed and operated by the University of California at Berkeley to measure the gas phase mixing ratios of a wide suite of volatile organic compounds (VOCs). The GC-MS-FID was configured to draw ambient samples from the measurement tower and measure C_3–C_6 alkanes, alkenes and alkynes, along with other VOCs, including aromatic, oxygenated and halogenated compounds at hourly intervals. This instrument, its deployment and results during the campaign are described by *Millet et al.* [2004]. The sampling was performed on the same tower using PTFE tubing.

[9] Also located at the Trinidad Head site was a Particle Into Liquid Sampler (PILS) [*Orsini et al.*, 2003; *Weber et al.*, 2001] coupled with ion chromatography (IC), which was operated by the Georgia Institute of Technology and the NOAA Pacific Marine Environmental Laboratory (PMEL). The PILS also sampled from the same height as the other instruments, although its inlet had a 1 μm cutoff cyclone, maintained at 56 ± 6% relative humidity (RH). Sodium carbonate and citric acid denuders were placed upstream of the instrument to remove gas phase acids and bases prior to sampling. The function of the PILS is to grow the sampled particles using steam and collect them into an aqueous sample flow through impaction. The IC analyzed the resulting solution in situ and yielded quantitative data on the total mass concentrations of water-soluble ions present in the ambient aerosols with a time resolution of thirty minutes.

3. Results

[10] The ARI and UMIST instruments were operated on averaging intervals of 2 and 10 min respectively, collecting both ensemble mass spectrum (MS) and size-resolved time of flight (TOF) data. The following data analysis products were all obtained using the methods described by *Allan et al.* [2003a, 2003b], unless stated otherwise. In those papers, an empirical correction factor was applied to the sulfate data, although the underlying reason was not known at the time. The evidence presented in this paper suggests that the correction arises from the need to account for nonunit particle collection efficiency, meaning a fraction of particles that are sampled into the AMS do not impact on the heated surface and are not detected. This appears to be due to the fact that nonspherical particles are not focused as well as spherical particles by the aerodynamic lens. The results of this study indicate that in this case, the collection efficiency effect for accumulation mode particles can be accounted for by multiplying the chemical mass concentrations by a correction factor of 2. This factor has been used in the calculation of all the mass loadings presented here, with the exception of sea salt. The data also includes corrections for the relative ionization efficiencies, as introduced by *Alfarra et al.* [2004], where each chemical mass concentration is divided by a factor to take account of the difference between the actual ionization efficiencies of the chemical species (measured in the laboratory or during routine calibrations) and the value assumed in the calculations based on the instrument's calibrated ionization efficiency. The values used for sulfate, nitrate, ammonium and organics are 1.15, 1.1, 4.95 and 1.4 respectively.

[11] Figure 1 shows a typical averaged mass spectrum from the experiment, with the larger of the peaks labeled and identified according to the ions producing the signals. Sulfate presents the highest particulate peaks in the mass spectrum, showing five peaks (*m*/*z* 48, 64, 80, 81 and 98) as completely distinct from the surrounding peaks. There are many organic peaks, but unlike urban environments [e.g., *Allan et al.*, 2003b], there is negligible signal above about *m*/*z* 160. The pattern instead resembles those seen in other remote MBL sites, such as Gosan, South Korea during the Asian Aerosol Characterization Experiment (ACE-Asia) [*Topping et al.*, 2004] and at Mace Head, Republic of Ireland during the North Atlantic Marine Boundary Layer Experiment (NAMBLEX) (J. D. Allan et al., UMIST, unpublished field data, 2002). In all these cases, the majority of the organic signal is contained within the lower *m*/*z*'s, especially 43, 44 and 55. This pattern is taken to indicated a high degree of chemical oxidation in the organics, which is expected, given the distance from major pollution sources and in agreement with the observation that the organic to elemental carbon (OC/EC) ratios measured at the site during that period were consistently high (20.1, averaged over the entire period). *m*/*z* 91 is visible as a distinct peak, which is normally an indicator that some aromatic chemicals are present.

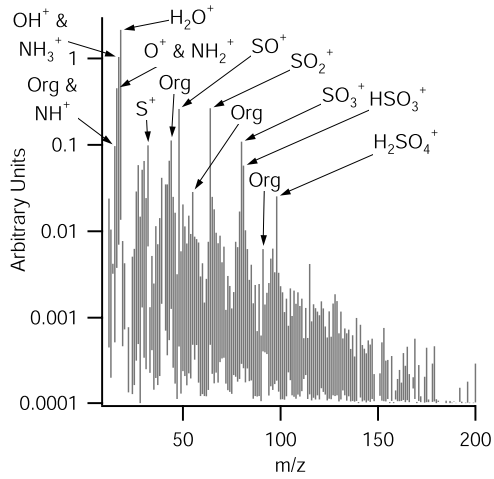

Figure 1. A typical mass spectrum from the data set, with the most significant peaks labeled. The contributions from gas phase material have been removed for clarity. Ammonium and sulfate dominate the major peaks of the spectrum. Although only a few major organic peaks have been labeled, most of the material represented by the peaks not labeled is organic. The majority of the organic signals are confined to the low *m*/*z* region of the mass spectrum.

[12] The example loadings shown in Figure 2 were obtained from the mass spectrum mode of operation of the instruments, which provides chemical mass concentrations in micrograms per cubic meter of air at ambient pressure as a function of time. The data from the ARI instrument were binned according to the difference between inlet temperature and the ambient dew point. This is discussed in much more detail below, but the sulfate, ammonium, organics and nitrate data shown in Figure 2 are hourly averages, using only the data from when the inlet temperature was at least 10°C greater than the dew point. Under these conditions, the particles were sampled relatively dry and therefore the established analysis techniques could be applied. The ammonium, sulfate and organic data reported from the UMIST instrument are not used for the general scientific discussion in this paper, due to the fact that its vaporizer and ionizer configuration affected the relative sensitivities of the different species in a manner not accounted for by the standard calibrations; the temporal variations reported for these species qualitatively agree with those of the ARI instrument, but the absolute loadings disagree by factors of around 1.5. However, this is partly

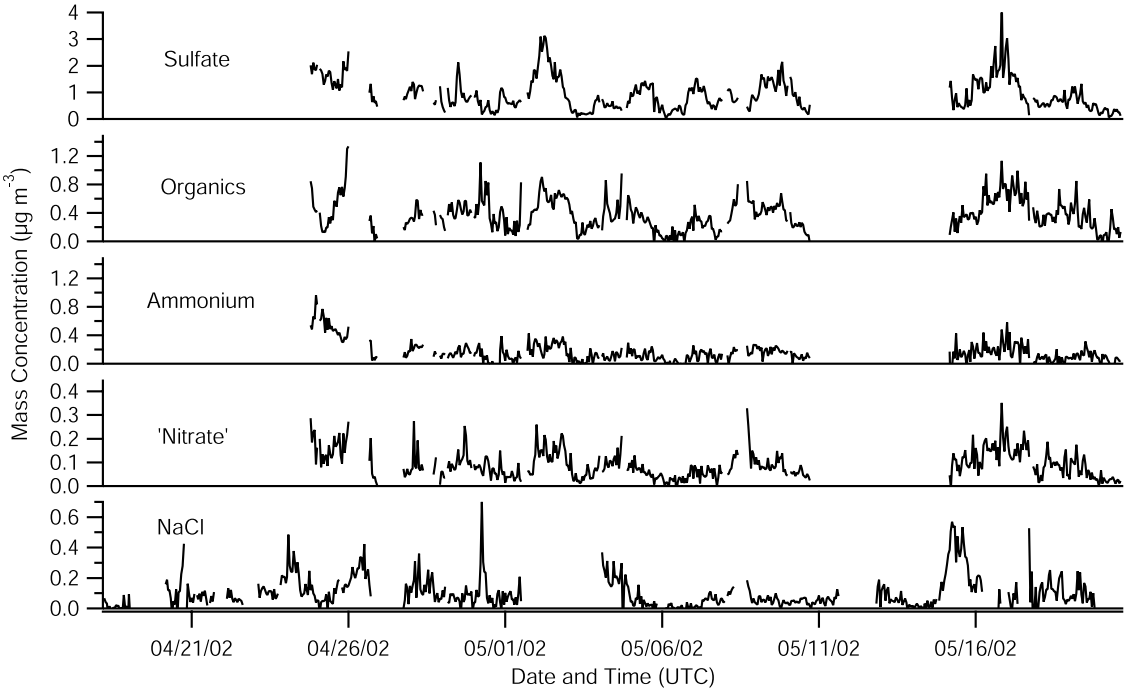

Figure 2. Hour-averaged total mass concentrations, derived from the MS mode of operation. The data are from the ARI instrument during temperature cycling, when the difference between inlet temperature and the dew point was greater than 10°C, as this is closest to the established protocol and has the fewest uncertainties (prior to 25 April the instrument was operated in dry mode only). The exception is the NaCl, which is taken from the UMIST instrument. The data referred to as "nitrate" may include organic nitrogen in addition to NO_3^+, as discussed in section 4.2.

expected because the UMIST instrument was optimized primarily for sea salt and it was anticipated that the other species would be compromised, so the ARI instrument is deemed more reliable for these.

[13] Ammonium loadings were calculated using the signals at *m/z* 16 and 17 and measured calibration values. These channels normally contain large contributions from gas phase oxygen and gas and particle phase water (O^+ and OH^+ ions), so these had to be subtracted numerically, based on other *m/z* channels and known fragmentation patterns. This technique will be described in more detail by Delia et al. (Particulate Ammonium from Aerodyne Aerosol Mass Spectrometer Measurements, manuscript in preparation, 2003). The overall composition of the particles is dominated by sulfate and organics, with mean average loadings of 0.93 and 0.38 μg m^{-3} respectively. There was very little nitrate, which had an average concentration of 0.09 μg m^{-3} and was rarely above 0.3 μg m^{-3}. Ammonium loadings, which averaged at 0.16 μg m^{-3}, were relatively low and did not always reach the amounts necessary to fully neutralize the sulfate present; the ratio of the averaged ammonium and sulfate loadings was 17.2% by mass, as opposed to the 37.5% required to achieve a 2:1 molar ratio.

[14] The sodium chloride loading was derived from the UMIST AMS and calculated by summing the signals at *m/z* 23 (Na^+), 35 (Cl^+), 36 (HCl^+) and 58 ($NaCl^+$), after subtracting any signals due to gas-phase components (e.g., $^{36}Ar^+$). The contributions of fragments containing the ^{37}Cl isotope were predicted from the intensity of the other peaks, assuming an isotopic ratio of 3.13:1 [*Coplen et al.*, 2002]. Tests with atomizer-generated particles using both pure sodium chloride and sea salt solutions showed that there were no significant peaks from NaCl at higher *m/z*'s to be expected. The measured mass loadings at Trinidad Head were fairly low, averaging at 0.1 μg m^{-3}. Note that the reported concentrations are likely to be only a fraction of the total suspended sodium chloride present in the atmosphere, as most of it will exist in coarse particles, which are not measured with 100% efficiency due to the low transmission efficiency of the aerodynamic lens above 800 nm [*Jayne et al.*, 2000; *Zhang et al.*, 2002] and the 2.5 μm cutoff of the cyclone. Also note that this particular chemical species is measured with a very low signal-to-noise ratio, due to the high background levels in the instrument and the relatively long vaporization times. The data must be averaged over large time periods to obtain meaningful results at the analysis stage, especially when dealing with the time of flight data.

[15] The particle time of flight data in Figure 3 show that there was an accumulation mode at vacuum aerodynamic diameters of around 300 to 400 nm, consisting mainly of sulfate, ammonium and organics. The modal diameter of the accumulation mode varied little during the experiment and was consistent between the four species, implying internal mixing, although nitrate has some presence in the supermicron regime and the organics show a small amount of signal below 100 nm. While the AMS on its own cannot directly prove the case for internal as opposed to external mixing, chemicals exhibiting common modal diameters for the duration of a campaign do present a strong case [*Allan et*

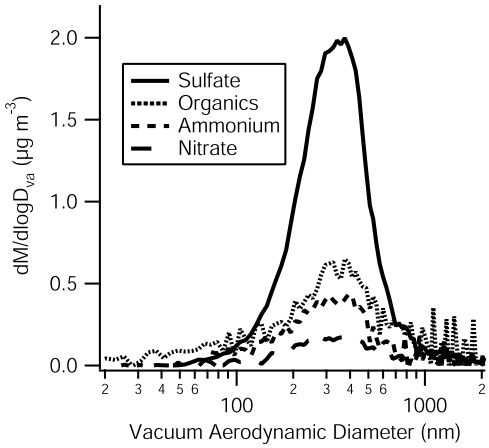

Figure 3. Averaged mass concentration as a function of vacuum aerodynamic diameter for the high $t - t_d$ sampling. The modal diameter stayed at around 300–400 nm for most of the experiment.

al., 2003b]. Conversely, the sea salt distribution was broad and stretched into the coarse mode (Figure 4), implying an external mixture with the other chemical components.

4. Instrumentation Issues

4.1. Behavior With Changes in Inlet Humidity

[16] As mentioned earlier, to facilitate the interpretation of the data from the ARI instrument, the data were separated according to the difference between the inlet temperature (at the critical orifice) and the ambient dew point ($t - t_d$) and then averaged into 1 hourly periods. The two data series presented in this paper are for when the difference was less than 5°C and greater than 10°C. These cut points were chosen because with the equipment used, the pinhole temperature spent the majority of its time in one of these two

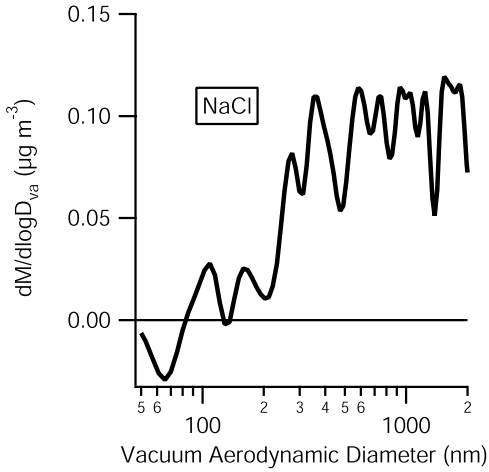

Figure 4. Mass distribution of sodium chloride. These data featured an inherently large amount of random noise, caused by the high background levels in the instrument. For this reason, the graph has been smoothed for clarity. The modal diameter is greater than 1 μm, above which quantification becomes difficult due to the size-dependent collection efficiency of the instrument.

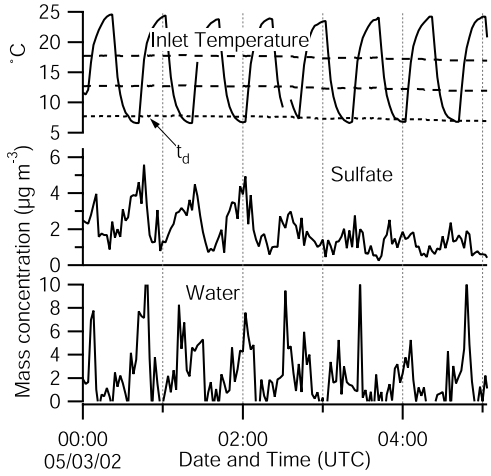

Figure 5. Graph showing the temperature cycling and the effect it has on the sulfate and water loadings. The ambient dew point (t_d) is also shown. The dashed lines above it indicate the t_d + 5°C and the t_d + 10°C values. As the temperature approaches the dew point, the reported sulfate and water loadings increase, due to the particles deliquescing and becoming more focused.

conditions, with rapid transitions between them (Figure 5). The large changes in measured mass concentrations also occurred at this point. 5°C above the dew point corresponded to an RH of around 71%, although the line leading to the inlet would have been cooler, due to a temperature gradient generated by conductive heating from the instrument. Therefore the highest relative humidity that the particles would have experienced would have been higher (a decrease of only 2°C would increase the RH to 81%). While it is accepted that the configuration used is a very crude method of studying particle hygroscopic behavior, the setup used in this experiment did not have sufficient accuracy in the temperature and humidity measurements to permit a more thorough analysis.

[17] When comparing the $t - t_d < 5$°C mass concentrations (low difference) with the corresponding $t - t_d > 10$°C (high difference) data, the low difference data are greater by a factor of approximately 2. This enhancement can also be seen in the averaged TOF data, but while there is an increase in the mass loading of the chemicals, there is no significant change in the vacuum aerodynamic diameters of the modes. When looking at this enhancement factor as a function of diameter, sulfate, ammonium and the organics are all enhanced by a factor of two at the modal diameter (Figure 6). At lower diameters, the enhancement is smaller. Nitrate behaves slightly differently in that its enhancement is only around 1.5. Also, there is an apparent suppression of the nitrate loadings in the coarse mode when the temperature approaches the dew point.

4.2. Focusing Issues

[18] The behavior associated with inlet temperature and humidity is due to the fact that when the temperature approaches the dew point, the particles deliquesce and become liquid droplets, as opposed to the crystalline shapes they can adopt when in the solid phase. It would be reasonable to assume that in this case, the majority of the

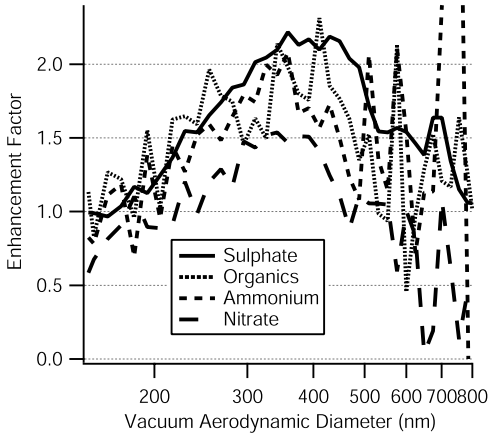

Figure 6. Enhancement factor as a function of diameter for the major species studied. Note that ammonium, sulfate and organics are enhanced by a factor of 2 in the accumulation mode. Sulfate continues into the slightly higher sizes, which is due to the fact that when the data are averaged over the entire experiment, sulfate has a larger presence in this regime relative to ammonium and organics. Nitrate is not enhanced as much in the accumulation mode and is actually suppressed as it approaches the supermicron regime.

accumulation mode mass is in the form of hygroscopic particles because they are composed principally of salts and organics that show some oxidation, which is in common with other remote marine environments [e.g., *Swietlicki et al.*, 2000]. It has been predicted that nonspherical particles will not focus as efficiently in the aerodynamic lens used in the instrument due to lift forces [*Liu et al.*, 1995a] but quantitative predictions for actual ambient particles have not been performed due to their complex nature. However, it has been consistently noted by many groups using AMSs that when dry, monodisperse particles are studied in the laboratory, the number of particles seen by the AMS compared to a Condensation Particle Counter (CPC) varies according to species (M. R. Alfarra, UMIST, unpublished lab data, 2002). The ratio of these counted numbers reflects the collection efficiency of the AMS. This collection efficiency is typically between 90 and 100% for dry ammonium nitrate particles, but the ratio is typically about 20 to 30% for ammonium sulfate.

[19] While other hypotheses have been proposed in the past for this phenomenon, it would be reasonable to suggest that when the ammonium sulfate particles dry in this situation, they form nonspherical shapes that do not focus very efficiently. Conversely, pure ammonium nitrate particles, while not necessarily spherical per se, do not form shapes that generate significant lift forces during focusing and acceleration. Lab experiments involving organic chemicals also show variations, with liquids such as oleic acid giving near 100% collection efficiencies and solids such as myristic, adipic and succinic acids giving lower ratios.

[20] The hypothesis that particle deliquescence improves focusing is supported by looking at the water measured by the instrument when compared to the inlet temperature. When the temperature is low and close to the dew point, the measured amount of water increases (Figure 5). The total mass of water in both the gas and particle phases entering the instrument is not altered by the inlet temperature but the majority of the gas phase material is removed by the skimmer [*Jayne et al.*, 2000], suggesting that water is condensing into the particle phase at temperatures close to the dew point. It also provides evidence that although the particles are exposed to very low pressures in the lens and the rest of the instrument, they do not have enough time to dry out completely. During periods of low inlet temperature, the particle numbers counted by the AMS in TOF mode [*Jimenez et al.*, 2003a] are similarly increased by a factor of around 2, confirming that the increase in observed mass is due to an increase in the number of particles detected rather than the amount of matter being detected on individual particles.

[21] It would be expected that as the particles take on water, the physical size of the particles must increase also, as seen by hygroscopicity tandem differential mobility analyzers (HTDMAs) [e.g., *Berg et al.*, 1998]. However, no noticable size change was observed with the AMS. Unlike DMAs, the AMS measures diameter aerodynamically and at a sufficiently low pressure that the particles sampled are in the free-molecular regime. This measured diameter is referred to as the "vacuum aerodynamic diameter" and varies linearly with particle effective density, which is proportional to the particle's density [*Jimenez et al.*, 2003b]. As a particle takes on water, its geometric (volume-equivalent) diameter increases, but if the solute is of a density greater than that of water, the overall density will decrease. For salts such as ammonium sulfate, any net changes to the vacuum aerodynamic diameter at subsaturated humidities will be insignificant, especially when considering the broad distributions presented here (J. L. Jimenez, U. Colorado at Boulder, personal communication, 2002). It must be noted that it is expected that some, but not necessarily all, of the water on the particles will evaporate between the critical orifice and the lens nozzle, so the aerodynamic diameter measured by the AMS is not necessarily the actual diameter at the high humidity (as also seen by *Buzorius et al.* [2002]). It is also difficult to predict what will happen as the temperature gets very close to the dew point, as some very large particle growth factors are possible. These issues add further uncertainties to the low $t - t_d$ sampling, which is why this data series was deemed unsuitable for use in the general scientific discussion.

[22] For the first time, this experiment has provided direct evidence that the detection efficiency of the AMS has a strong dependence on the shape and phase of the measured particles. Indeed, this explains the reason why an empirical correction factor has been needed in previous instrument comparisons [e.g., *Drewnick et al.*, 2003]. *Allan et al.* [2003a, 2003b] quoted the factor as being 2.5, but it has become apparent that part of this correction is due to several of the minor fragmentation peaks in the sulfate mass spectrum, such as *m/z* 18 (H_2O^+), 32 (S^+) and those due to the ^{34}S and ^{18}O isotopes, that were not directly used in the determination of the sulfate mass. When these are included, after appropriately accounting for the mass spectral interferences at these fragments from other species (as has been done in this case), the necessary factor is reduced from 2.5 to 2. It must be noted that in this case, the organics were likely to be mostly internally mixed within the

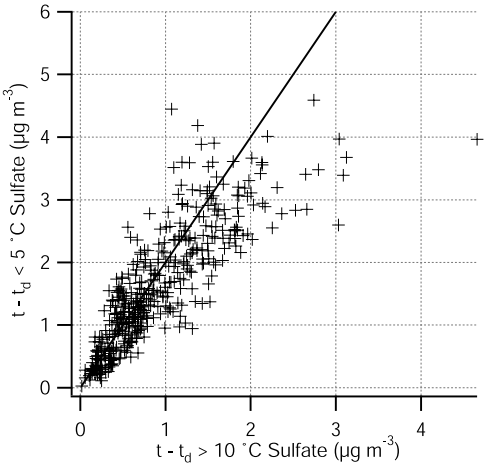

Figure 7. Graph showing the enhancement of measured sulfate loadings due to deliquescence. The line shows the factor of 2 assumed in other studies. There are departures on the right hand side of the graph, which will be due to particles either not drying during high $t - t_d$ periods or not deliquescing during low $t - t_d$ periods.

accumulation mode. Through this and other studies, it seems that this factor of 2 applies to most data arising from ambient hygroscopic particles, which dominate the fine regime on this occasion. It is reasonable to assume that in most field deployments where temperature control is not used, the aerosols are sampled dry because the heat generated by the instrument's turbopumps conductively increases the temperature of the inlet assembly to above that of the cabin, which is often greater than the ambient temperature.

[23] The enhancement at low $t - t_d$ in the sulfate series in particular can be seen in the scatterplot in Figure 7. A line representing an enhancement factor of 2 is included as a guide to the eye. Most of the data points follow this line, with a few significant departures where the enhancement is lower. These outliers may be due to the detection of particles that had not effloresced at the higher temperatures, or not deliquesced at the low temperatures. Statistically, the enhancement averages at 1.93 with a standard deviation of 0.5, although the "true" enhancement is likely to be slightly higher as the mean is affected by the departures. There are also some smaller but less episodic variations present in Figure 7, which could either be due to random errors in the reported concentrations or variations in the dry particle morphology altering their focusing properties. While it would be desirable to take these variations into account explicitly, limitations imposed by the lack of overall signal mean that the random and systematic errors are not easily distinguishable, so a constant enhancement of 2 has been used. Despite being an approximation, other comparison studies such as *Drewnick et al.* [2003] have found using a constant correction factor to be quite robust.

[24] While it is accepted that limitations in the control and monitoring hardware used in this experiment hinder quantitative investigations into the hygroscopic behavior, the configuration gives some insights into the chemical nature and mixing state of particles present. For instance, during the experiment, the variations in the enhancements for sulfate, organics and ammonium are matched in their temporal behavior, except for one noticeable departure on 4 May, where the ammonium and sulfate enhancements increase to around 4 while that of the organics remained at 2. A discrepancy such as this can only be caused by the ammonium and sulfate being externally mixed with the organics during this period, as an internal mixture would mean the enhancements would be equal, supporting the case that they are largely internally mixed for the remainder of the time. The TOF distribution from this period showed a large sulfate mode present at around 200–300 nm, which is much smaller than the typical mode seen during the campaign. It is also interesting to note that the collection efficiency of laboratory-generated pure ammonium sulfate particles is normally around 20–30%, which would give an enhancement of around 4. As this occurred during a period of land-based influence (see section 5.3), it is most likely that further up the coast, there was a source of new particles composed mainly of ammonium sulfate with minimal contributions from organic chemicals.

[25] The issues discussed clearly present a challenge for future AMS use. Further work is needed to better quantify these effects and to validate field data obtained with the AMS, which will entail detailed laboratory experiments and possibly numerical simulations to properly understand these processes. However, from this albeit limited insight, it is clear that greater monitoring and/or control of the inlet temperature and humidity will have to be exercised in future. The routine use of a beam shape probe as used by *Jayne et al.* [2000] may also need to be considered, as it is desirable to actually know the collection efficiency at any one time rather than assume it. These measures have been implemented in more recent AMS deployments [e.g., *Allan et al.*, 2003c] and work to further study the physical phenomena is ongoing [e.g., *Matthew and Middlebrook*, 2003]. These will be presented in future publications.

5. Discussion

5.1. Inorganic Chemicals and Comparison With PILS-IC Data

[26] The observation of a large sulfate fraction of the total submicron mass and the single accumulation mode is consistent with other measurements of the MBL [e.g., *Raes et al.*, 2000]. The large sulfate to ammonium ratio implies that the particles were typically composed of more acidic compounds such as ammonium bisulfate (NH_4HSO_4) or methylsulfonic acid (MSA, CH_3SO_2OH), which again has been seen in other studies [e.g., *Quinn et al.*, 1993]. MSA has been found to give a mass spectral signature in the AMS similar to that of sulfate (L. Phinney and R. Leaitch, Meteorological Service of Canada, personal communication 2003), but as the loadings of MSA reported by the PILS-IC were on average 6.5 times less than that of nonsea-salt (nss) sulfate, the majority of the reported mass will be sulfate or bisulfate. Sources are likely to include oxidation of biogenic dimethylsulfide (DMS) [*Charlson et al.*, 1987; *Sharma et al.*, 1999] and the conversion of anthropogenic SO_2 to H_2SO_4. Eastern Asia is a major source of SO_2 [*Shrestha et al.*, 1996] and the conversion may take place either through oxidation in the gas phase or aqueous-phase processing within the MBL as the air masses travel over the Pacific Ocean.

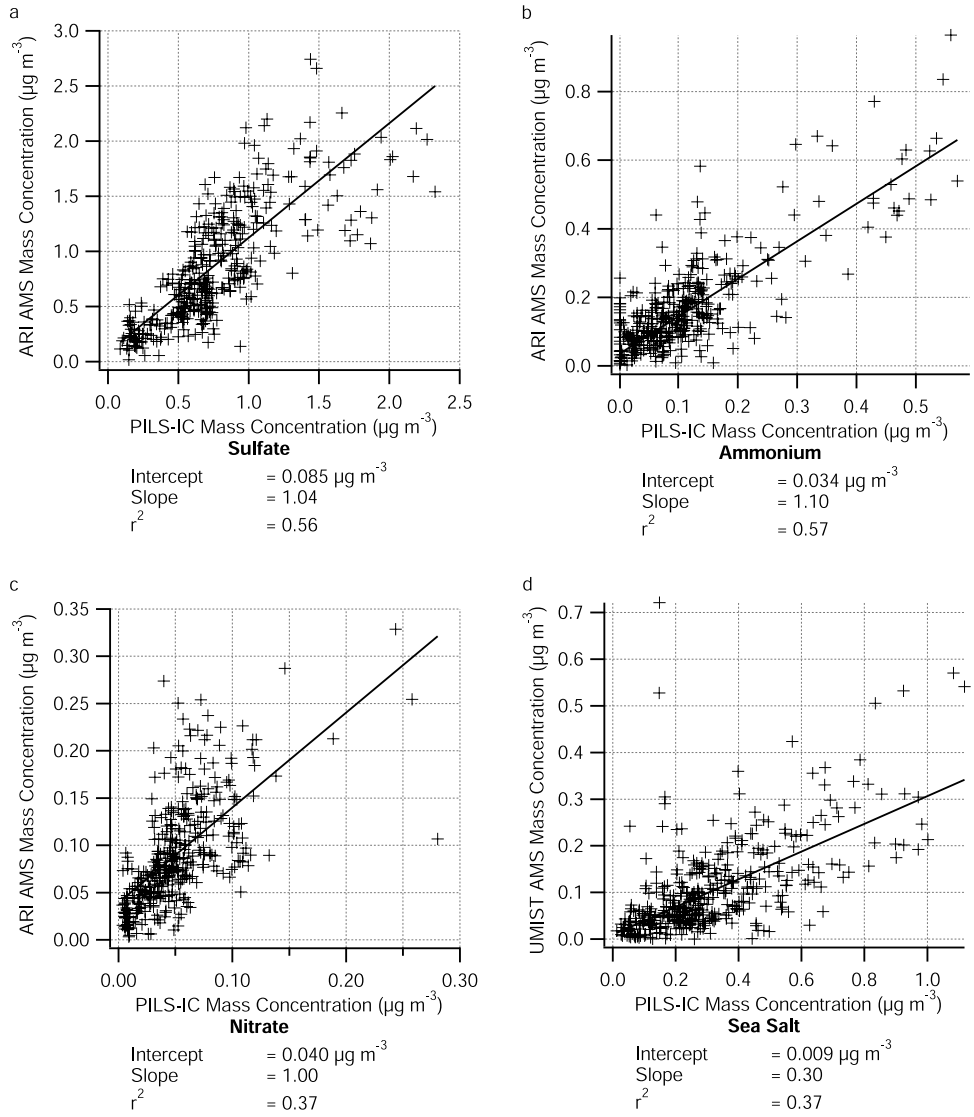

Figure 8. Scatterplots comparing the AMS-derived mass concentrations with those of the PILS-IC. All but the sea salt were taken from the ARI instrument under high inlet temperature conditions, as with Figure 2. Linear regression statistics are also shown. The slopes of the sulfate, ammonium and nitrate are favorable, as are the intercepts of the sulfate, ammonium and sea salt. It appears that the AMS was measuring sea salt at a reduced efficiency and an additional component was contributing to the AMS-reported nitrate.

[27] Comparisons between the total loadings measured with the AMS and the PILS-IC instrument have been performed on other occasions and have previously been very encouraging [*Drewnick et al.*, 2003; *Jimenez et al.*, 2003a], as many of the results from both instruments are directly comparable. Scatterplots comparing the results can be seen in Figures 8a–8d, along with the outputs of linear regression analyses. The AMS data used in this section, unless stated otherwise, are from the ARI high $t - t_d$ sampling (those presented previously in Figure 2). The 1σ detection limits due to the ion counting statistics in the AMS are calculated according to the method described by *Allan et al.* [2003a] and were found to be 0.005 μg m^{-3} for nitrate, 0.017 μg m^{-3} for sulfate, 0.045 μg m^{-3} for ammonium and 0.018 μg m^{-3} for sea salt. The PILS-IC has a relative standard error of between 5 and 7% for all ions.

[28] The measured PILS-IC and AMS sulfate compares very well, giving a slope of 1.04 and a relatively small intercept of 0.085 μg m^{-3} and the ammonium compares with a slope of 1.10 and an intercept of 0.0034 μg m^{-3}. The r^2 values are not very high at 0.56 and 0.57 respectively, but the discrepancies do not seem to follow any systematic pattern. This random error will partly be due to the lower signal-to-noise ratios of the AMS data compared to those of the PILS-IC, but variations in the AMS particle collection efficiencies (seen in the variations in the enhancements) may also contribute to the discrepancy.

[29] The sea salt mass concentrations measured by the PILS-IC are greater than those measured by the AMS by a factor of around 3. There will almost certainly be losses in the AMS because sodium chloride tends to form cubic crystals in the solid phase, which will not focus very well

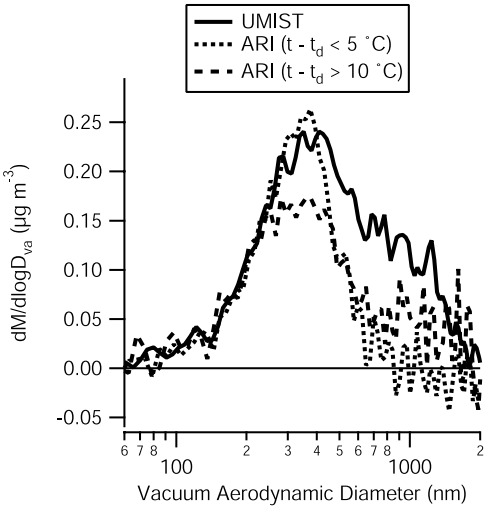

Figure 9. An example of nitrate as a function of aerodynamic diameter, as seen by the two instruments and the two inlet conditions of the ARI instrument. Note the fact that the UMIST instrument sees more than the ARI instrument above 300 nm, due to its higher vaporizer temperature being able to vaporize the sea salt particles fully. Also note that with the ARI instrument the low inlet temperature enhances the accumulation mode loading but suppresses the coarse mode.

in the aerodynamic lens. This hypothesis is reflected in the calibration data, where a collection efficiency of only 17% was achieved for sodium chloride. However, ambient sea salt particles are not expected to possess the same structure as the calibration particles, due to differences in their composition and generation mechanism, therefore the "true" collection efficiency of the detected particles may be different. The AMS/PILS-IC comparison suggests it is around 33%, but this does not take into account the fact that the two instruments' upper size cutoffs are within the regime in which the majority of the sea salt mass resides ($\approx$1 μm). The differences in the cutoff functions will lead to a discrepancy of some description, but this will be very difficult to predict.

5.2. Nitrate Issues

[30] The one major source of disagreement between the PILS-IC and the AMS is the reported nitrate, in which the AMS generally measured more. The regression reports an intercept of 0.04 μg m^{-3}, which is high relative to the mass concentrations measured and the standard errors associated with the instruments. The scatterplot shows significant departures from the fitted line that do not appear to resemble purely random noise, which coupled with the fact that the slope is close to unity (1.004), suggests that the AMS and PILS-IC are observing the same amounts of ionic nitrate but the AMS is measuring another chemical species in addition to this. A similar discrepancy was found by A. M. Middlebrook et al. (NOAA Aeronomy Laboratory, unpublished field data, 2003) off the east coast of the USA during the New England Air Quality Study (NEAQS), aboard the research vessel Ronald H. Brown.

[31] In addition to the accumulation mode, the UMIST instrument observed an additional nitrate mode in the coarse regime (Figure 9). Previous work, mainly at continental locations, has shown that signals at *m/z* 30 and 46 are dominated by the NO^+ and NO_2^+ fragments, which are typically around the ratio 2.5:1 for ammonium nitrate. However, during this experiment, the ratio of the signals is far greater than this at averages of 5.3 and 6.8:1 for the ARI and UMIST instruments respectively, suggesting that ammonium nitrate is unlikely to be the major source of these signals. The average ratio of the signals in *m/z* 30 and 46 for the UMIST instrument is larger in the coarse mode than the accumulation mode (Figure 10). A high ratio can be indicative of the presence of mineral nitrates such as $NaNO_3$ and $Ca(NO_3)_2$, which is consistent with the fact that the coarse mode nitrate is not seen very strongly by the ARI instrument; its vaporizer was operated at too low a temperature to fully vaporize mineral nitrates. *Topping et al.* [2004] concluded that during ACE-Asia, some chloride was being displaced from the sea salt particles through nitric acid deposition. Nitric acid deposition onto dust particles was also postulated, forming $Ca(NO_3)_2$, which cannot be directly discounted in this case, as even the UMIST vaporizer was not hot enough to permit the study of crustal elements such as calcium. While some sulfate is also expected to be present in the sea salt particles and may indeed be reflected in the data, it is dwarfed by the observed sulfate in the accumulation mode and is not distinguishable.

[32] As a case study two periods were chosen where there was a significant difference in the molar ratio of sodium and chloride ions, as seen by the PILS-IC. The mass distributions for these periods can be seen in Figure 11. Note that for the purpose of these graphs, the correction for beam defocusing has not been applied to either nitrate or the sea salt, as the true collection efficiency for these large sea salt particles is not known. The top graph shows an averaged trace from 17:00 UTC on 24 April 2002 until 01:30 on 26 April, where the molar ratio of chloride to sodium ions averaged 0.67. During this period, significant amounts of nitrate can be observed and the ratio of the integrated supermicron nitrate mass to sea salt is roughly 1.2. Conversely, during the period of 06:00 until 21:00 UTC on

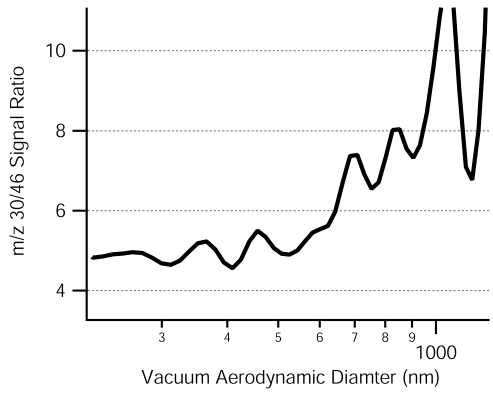

Figure 10. *m/z* 30/46 signal ratio as a function of aerodynamic diameter, as seen by the UMIST instrument. The change observed as the diameter increases indicates a change in the nature of the nitrate, possibly from NH_4NO_3 to $NaNO_3$. The values outside the diameter range of this graph are too noisy to be of use.

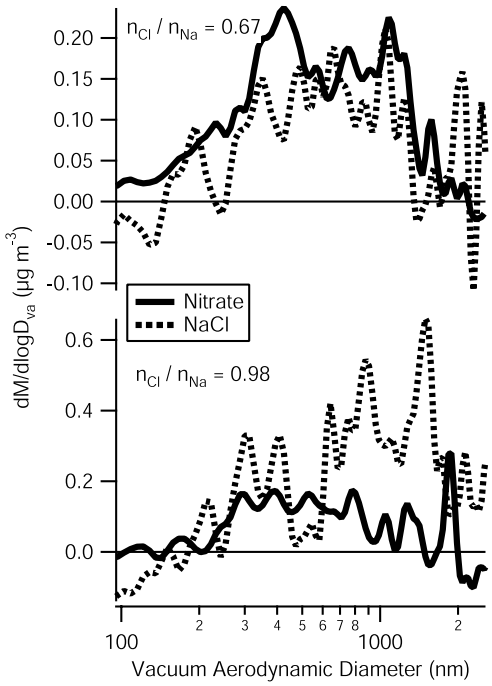

Figure 11. Comparison of size-resolved nitrate and sodium chloride mass distributions. The first period (4/24/2 17:00–4/26/2 1:30) is when the PILS reported a low molar ratio between chloride and sodium, during which time the AMS reported significant coarse mode nitrate. During the second period (4/26/2 6:00–21:00), the molar ratio was higher and less coarse mode nitrate was observed relative to the sea salt.

26 April 2002, when the molar ratio was 0.98, the supermicron mass ratio was only 0.13.

[33] The lower enhancement factor in the nitrate seen previously in Figure 9 could be a manifestation of the presence of more than one form of nitrate being observed, which seems to be the case. The apparent suppression of the coarse mode at low inlet temperature is probably due to the way the larger particles are lost in the inlet assembly of the AMS. It has been predicted using computational fluid dynamics that particles larger than around 0.7 to 1 μm will be lost due to impaction with the inner walls of the tubing as they leave the pinhole, with the effect being more pronounced for particles with larger aerodynamic diameters (X. F. Zhang, Aerodyne Research Inc., personal communication, 2002). However, what the computer model does not take into account is the fact that particles may bounce when they hit the wall and become re-entrained in the airflow. *Topping et al.* [2004] reported loadings at particle sizes of around 2 to 3 μm, which are larger than the theoretical limit predicted by the computer model, so it is probable that much of the particles seen around and above a micron are ones that have bounced at some stage.

[34] If this phenomenon is real and significant, it would be expected that aqueous particles will be less likely to bounce off the stainless steel tubing than dry ones, offering a reason why the coarse mode nitrate loading is suppressed instead of enhanced when the temperature approaches dew point. Also, the spray effect at the pinhole that causes the impaction of the particles occurs at a higher pressure than the nozzle acceleration, so is more dependent on the "classical" aerodynamic diameter of the particles. Unlike the vacuum aerodynamic diameter, this is less dependent on particle density and therefore increases as particles grow hygroscopically, thereby increasing the impaction rate. Sea salt-based particles will be more susceptible to this effect than the sulfate-based particles, as they are known to grow more at high humidities [*Berg et al.*, 1998]. The accumulation mode nitrate's enhancement factor is apparently less than that of the other components, which is probably due to the bimodality of the nitrate distribution and the enhanced accumulation mode crossing over with the suppressed coarse mode distribution.

[35] However, returning to the comparison between the AMS and the PILS-IC, the presence of sodium nitrate is unlikely to be the source of the nitrate discrepancy, as the PILS-IC should measure that component as well. Also, given that the AMS detects sea salt with a reduced efficiency compared to the PILS-IC, a negative artifact would be expected in the AMS data if this effect were significant. There is a nitrate peak in the AMS size distribution that occurs at the same diameter as the sulfate, ammonium and organics, at around 300 to 400 nm. However, the ratio of the *m/z* 30 and 46 signals is around 5, which is still too high to be purely ammonium nitrate. One other potential source of this signal is the amine family of compounds, which can give a strong signal at *m/z* 30 (due to the $NH_2CH_2^+$ or $NHCH_3^+$ fragments), with little signal at 46 (M. R. Alfarra, UMIST, unpublished lab data, 2002), but other chemicals such as organic nitrates cannot be ruled out, as some of these are documented as having peaks at *m/z* 30 in standard 70 eV mass spectrum libraries [e.g., *Linstrom and Mallard*, 2003]. Detailed laboratory characterizations of the fragmentation patterns of particulate organic nitrates in the AMS have not yet been performed and will have to be carried out in the future. These nitrogen-bearing organic species would not produce nitrate ions in solution and would therefore not be detected as such by the PILS-IC. The hypothesis that one or more nitrogen-containing organic chemicals are responsible for the discrepancy is strengthened by the analysis shown in Figure 12, where the differences between the nitrate concentrations reported by the AMS and the PILS-IC are plotted against the AMS-reported organics. There is a degree of positive correlation shown by the linear regression (r^2 = 0.27), with an intercept close to zero (-0.002 μg m^{-3}), suggesting that the extra nitrate reported by the AMS is somehow linked to the organics in the particle phase.

[36] While the precise source of the discrepancy cannot be identified in this analysis, it would seem that the term "nitrate" should be treated as a very general term in this experiment, as there appears to be at least three separate contributions to the reported chemical loadings, being ammonium nitrate in the accumulation mode, sodium nitrate in sea salt particles and potentially one or more nitrogen-bearing organic chemicals. The excess nitrate reported by the AMS over the PILS-IC was also compared with gas phase NO_y data taken at the site, but only a very weak correlation was found (slope = 0.0225 μg m^{-3} ppb^{-1}, intercept = 0.023 μg m^{-3}, r^2 = 0.078). Using the ideal gas

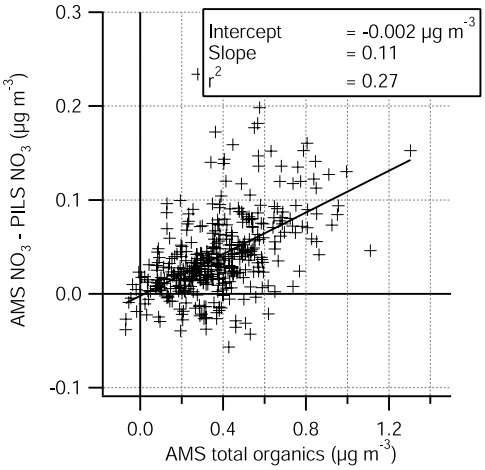

Figure 12. Scatterplot comparing the discrepancies between the AMS and the PILS-IC reported nitrate and the organics reported by the AMS. The regression shows a relationship with a small intercept, supporting the hypothesis that nitrogen-containing organic chemicals are responsible for the extra nitrate reported by the AMS over the PILS-IC.

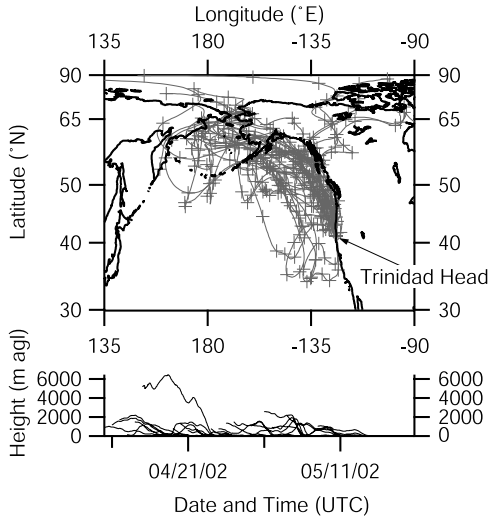

Figure 13. HYSPLIT 10-day back trajectories. Check marks are shown at one-day intervals and the trajectories are repeated every 24 hours. The general direction of approach is from the northwest, with the majority of air masses originating from the northern Pacific region. There is some variation in the final 24 hours of the air histories.

law and assuming standard temperature and pressure and a parent molecular mass of 30 amu, the particulate mass concentration can be converted to a molar mixing ratio, which corresponds to a slope of 0.018 when compared to the NO_y data. As the parent molecules are almost certainly more massive than the 30 amu used, the above provides an upper estimate of the total mixing ratio of nitrogen-containing particulate organics, which is small (<1.8%) compared to the total NO_y budget.

5.3. Air Histories

[37] Back trajectories were calculated using the HYSPLIT model (R. R. Draxler and G. D. Rolph, HYSPLIT (HYbrid Single-Particle Lagrangian Integrated Trajectory) Model access via NOAA ARL READY Website, http://www.arl.noaa.gov/ready/hysplit4.html) and are shown in Figure 13. These each cover ten days prior to arrival at the site and are separated by 24 hour intervals. According to the analysis, at any one time, the air sampled at Trinidad Head had spent most of its previous 10 days over the northern Pacific and Arctic regions. However, the 48 hours or so prior to sampling was more variable, with influences from other coastal areas of the United States on certain occasions, which gave rise to some of the variations in the particles seen. An example of the difference is shown in Figure 14. On 6 May, the air came directly from the west, over the Pacific Ocean and the particles were distributed in a single, roughly lognormal mode. Conversely, on the 24 April, the air spent much of the previous 24 hours over the coastal regions of Washington and Oregon. When comparing the two periods, there is a much greater amount of particulate matter during the period with coastal influences (an increase reflected in the PILS-IC data). The change in the organics is particularly noticeable below 100 nm; during the clean periods there is very little mass of any species in this regime. When the AMS has been deployed in urban environments, a large and distinct organic mode linked to traffic emissions is ubiquitously seen at theses sizes [e.g., *Allan et al.*, 2003b], so this is the most probable source. However, also note that the mode diameter of the accumulation mode particles increased to 400–500 nm, which

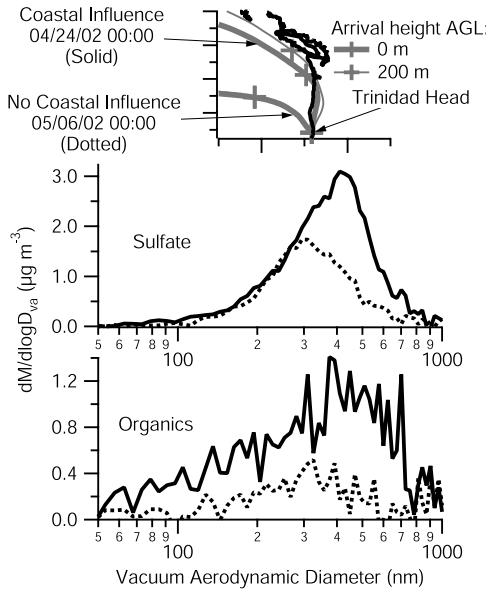

Figure 14. Comparison of size-resolved organic and sulfate data from two different back trajectory periods, comparing a period of open ocean fetch with one spending much of the previous 24 hours over land. The check marks on the trajectories indicate the 24-hour points. The back trajectory analysis was repeated at different heights and the arrival route was found to be largely invariant of the finishing height. The trajectories corresponding to 0 and 200 meters above ground level (AGL) are shown. The modal diameter increased and extra particulate matter, the organics in particular below 100 nm, was present when the air had coastal influences.

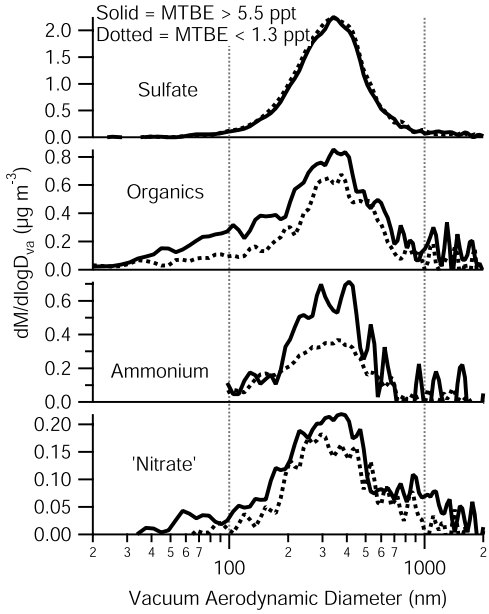

Figure 15. Comparison of the averaged size-resolved mass distributions of nitrate, sulfate, organics and ammonium based on ambient MTBE concentrations for the purpose of comparing data from periods of coastal influence to those without. The data used were those during periods when the concentration was below its lower quartile (less than 1.3 ppt) or above its upper quartile (greater than 5.5 ppt). The sulfate was largely invariant but the ammonium and nitrate modes were increased in magnitude by the presence of land-based emissions. The ammonium data below 100 nm is deemed invalid due to gas phase interference to the *m*/*z* channel used (16). The organic loading also increased, mainly around sizes of 100 nm, which will be due to traffic emissions.

implies that much of the extra mass is gas-phase material adsorbing onto and growing the preexisting MBL particles rather than purely being in the form of new particles.

[38] Coincident activity in the MTBE time series as measured by the GC-MS-FID confirms that traffic emissions are present in the air sampled. As discussed in section 5.3, this is a fuel additive that is emitted directly into the atmosphere by vehicles and has a relatively short lifetime in the atmosphere, so can be used in this analysis to indicate the presence of fresh pollution emitted within North America [*Millet et al.*, 2004]. According to the back trajectory analysis, at any one time, a given air mass sampled had spent at most two days over populated areas of the North American coast prior to reaching the site. To systematically compare the locally influenced air with the "clean" Pacific air, separate, averaged size-resolved mass distributions were generated for periods when the MTBE concentrations were below their lower quartile (1.3 ppt) and above their upper quartile (5.5 ppt) levels and are shown in Figure 15.

[39] This analysis shows that on average, the sulfate was unaffected in the shape of its distribution, despite incidental changes such as that discussed above. The average magnitude was actually reduced by 5.3% during periods of elevated MTBE. The overall reduction could be due to deposition of the MBL sulfate after reaching the coast, but a difference this small could simply be a chance finding. Nitrate and ammonium saw increases of 44 and 59% in their magnitudes, but their shapes and mode diameters remained similar. The increase in ammonium will be due to the fact that there are more significant sources of ammonia over land than sea (both biogenic and anthropogenic) that will quickly be taken up onto the acidic sulfate-containing particles from the MBL. The increase in nitrate may be due to nitric acid depositing from the gas phase on the particles once the ammonia has sufficiently neutralized the particles but an increase in the ammonium nitrate fraction would be reflected in a relative decrease in the ratio of the average signals at *m*/*z* 30 and 46 toward around 2.5. When calculated, this ratio actually increases from 5.4 to 7.3, implying that the additional perceived nitrate is mostly in the form of mineral nitrates or nitrogen-bearing organics instead. The organics, on average, increased by 56% during periods of high MTBE concentrations, partly due to the increase in traffic activity at around 100 nm. However, there also appears to be additional material in the larger sizes as well, which is probably organic chemicals depositing onto the accumulation mode particles from the gas phase. These could be processed VOCs of either biogenic or anthropogenic origin, as sources of both exist on land.

5.4. Comparison of Particulate Organics With Gas Phase VOCs

[40] As discussed before, the overall mass spectral signature of the organics present shows high signals in the low *m*/*z*'s, with particularly high signals at *m*/*z* 43, 44 and 55. This signature can be interpreted as heavily aged organic chemicals, as has been observed at other remote sites. However, it would be expected that episodes of younger and therefore less oxidized organic species be observed in this study, both due to shipping activity and emissions from coastal regions.

[41] This experiment presented a good opportunity to compare quantitatively the organic chemicals observed in the particle phase with the AMSs and those in the gas phase observed with the GC-MS-FID. When qualitatively comparing simple time series, similarities can be noted with the total AMS-measured organic loading and the concentrations of tracers measured with the GC-MS-FID. Figure 16 shows, as an example, a comparison with MTBE and benzene. As discussed by *Millet et al.* [2004], both are directly emitted from gasoline and by motor vehicles and subsequently degrade in the atmosphere, largely as a result of OH oxidation, at different rates. Using measured reaction rates and assuming an OH concentration of 10^6 molecules cm^{-3}, MTBE has an estimated chemical lifetime (k^{-1}) in the atmosphere of around 3.6 days [*Wallington et al.*, 1989], whereas that of benzene is approximately 9.7 days [*Semadeni et al.*, 1995]. The downward trend in the benzene data during the experiment is the seasonal benzene cycle that is ubiquitous of long-lived hydrocarbons in the northern mid latitudes [*Goldstein et al.*, 1995; *Jobson et al.*, 1994]. Particulate organics are typically generalized as being composed of primary and secondary components, the former being formed at the source, with the latter arising due to chemical reactions that transfer material

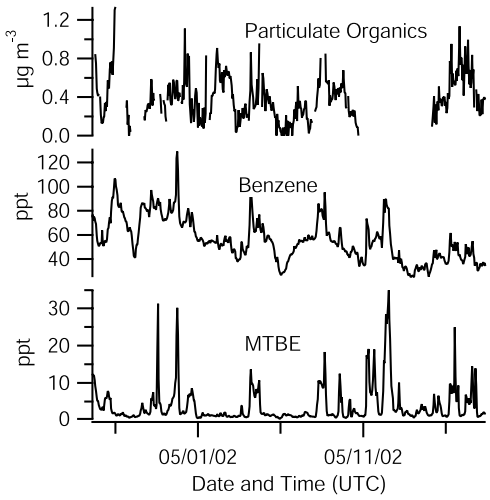

Figure 16. Comparison of total particle phase organics with gas phase Benzene and MTBE, measured using the GC-MS-FID. Upon visual inspection, similarities can be noted between the particulate organics and both gas phase species.

from the gas phase. Chemically aged VOCs have lower vapor pressures and will adsorb onto particles, adding to their mass and size, and may also undergo subsequent oxidation in the particle phase.

[42] Linear covariance analysis [*Press*, 1992, equation (14.5.1)] was performed to quantitatively compare the two data sources and determine which components were most closely linked in the time series. This analysis was applied to the entire data series at once, made possible by the similarities in the air histories, as shown by the back trajectory analysis; there were no sudden air mass history changes that would have created large positive or negative artifacts in the comparisons. The AMS data used are those from the ARI instrument during low inlet temperature sampling, as this is thought to have the highest signal-to-noise ratio and not be subject to as much chemical thermal fragmentation as the UMIST instrument. However, when the analyses were repeated for the UMIST instrument and the ARI high inlet temperature time series, they produced qualitatively similar results.

[43] When the total loading of particulate organics is compared to the different gas phase components (Figure 17), a positive correlation is noted with most gas phase species, with the hydrocarbons having the strongest relationship. While the majority of chloroform in the atmosphere is biogenic in origin [*Laturnus et al.*, 2002], it has a long atmospheric lifetime (112 days using the conditions assumed above [*Atkinson et al.*, 1997]), so most of the fluctuations seen will mainly be due to anthropogenic emission events, hence the strong relationship to the particle phase organics. There is little correlation with DMS, which is to be expected, as this is not a significant source of organic carbon and does not share a common source with the particulate organics. There is an anticorrelation with acetonitrile, possibly because lower acetonitrile concentrations are indicative of oceanic uptake and suppressed mixing within the atmospheric boundary layer (as postulated by *Millet et al.* [2004]), under which conditions the particulate organic concentration at the ground will be elevated.

[44] Further information can be gathered by looking at the contribution to the organics from particular *m*/*z*'s. The fraction of the total organic loading that exists at *m*/*z* 44 can be taken as an analog of the level of oxidation in the organics. This specific peak is very strong in the mass spectra of heavily oxidized organic chemicals such as di- and poly carboxylic acids [*Alfarra et al.*, 2002] and has been used to characterize particulate organics in other field studies [e.g., *Allan et al.*, 2003b]. When the covariance analysis against the gas phase VOC is repeated using the logarithm of this ratio, the strongest relationship is observed with oxidized species such as aldehydes and ketones (Figure 18), which are the products of photochemistry in the gas phase. Weak anticorrelation is noted with the hydrocarbons and a stronger anticorrelation with the short-lived combustion species, such as the methylbenzenes, is observed. Note that none of the covariance values are particularly large, but this is mainly due to the low organic mass loadings in the particle phase and the inherent amount of random noise in the time series. Conversely, if the analysis is repeated for the fraction of *m*/*z* 57 (Figure 19), which is known to be very prevalent in primary organic particles emitted by motor vehicles [*Allan et al.*, 2003b; *Canagaratna et al.*, 2003], the order of the gasses is reversed, with the short-lived combustion tracers correlated and the oxidation products anticorrelated.

[45] This comparison offers an entirely self-consistent view of the behavior of the organic chemicals in the particle phase. The analysis gives direct evidence that the oxidized organic species tend to dominate in the particle phase when the air has undergone sufficient photochemical ageing since the emission of the organic precursors. Conversely, during times of high gas phase concentrations of less oxidized chemicals and short-lived combustion tracers, the less oxidized species have more of a presence in the particle phase.

[46] Correlation is seen between α-pinene and isoprene and the *m*/*z* 57 fraction because these are produced biogenically in forests and will therefore be more prevalent in air that has spent significant time over land, which will also contain more primary organics due to traffic emissions. There are no apparent relationships with acetonitrile, meaning that while its behavior is reflected in the overall loading of particulate organics, it does not affect their composition, strengthening the above hypothesis that an atmospheric mixing effect is largely responsible for the temporal behavior of acetonitrile.

6. Conclusions

[47] Two AMSs were deployed and operated at Trinidad Head during ITCT 2K2 to study the physical and chemical properties of submicron particles in the marine boundary layer. One was modified to be able to vaporize sodium chloride particles, while the other was operated with a temperature-controlled inlet.

[48] The accumulation mode particles were consistently found in a single distribution of a vacuum aerodynamic diameter of around 300 to 400 nm and the nonrefractory component was composed principally of sulfate, ammonium

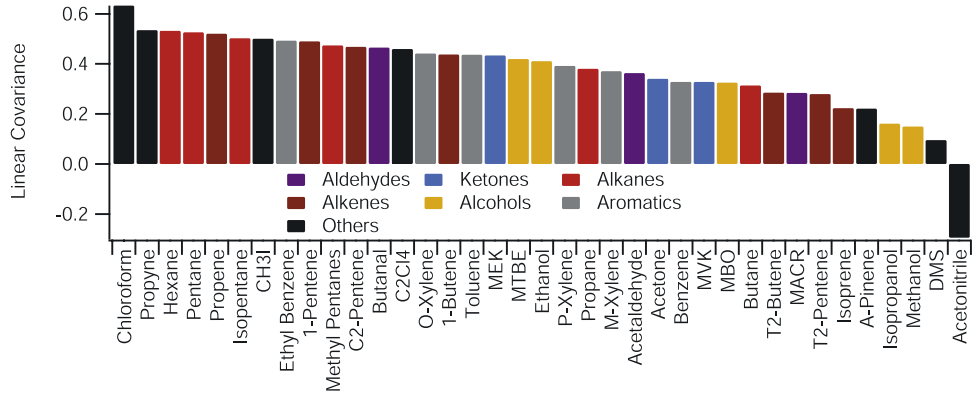

Figure 17. Output of the linear covariance analysis, comparing the mixing ratio of various VOCs with the total mass concentration of particulate organics. The species with the strongest positive relationship with the total particulate organic loading are on the left, with the weakest on the right. Positive covariance is seen with most species.

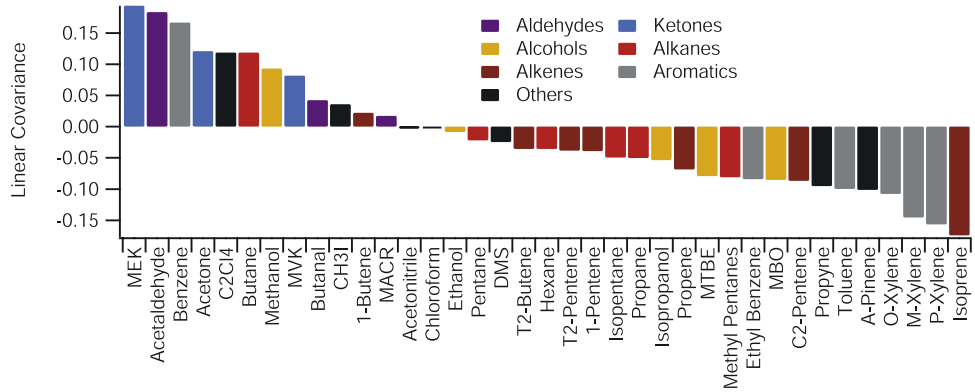

Figure 18. Covariance plot of the *m*/*z* 44 ratio to the total organics, which can be taken as an analog of the level of oxidation in the particle phase organics. A positive relationship is shown with the heavily oxidized VOC species such as the aldehydes and ketones, with a negative relationship with the short-lived combustion tracers. This shows the particulate organics are most oxidized during periods of high ageing in the gas phase.

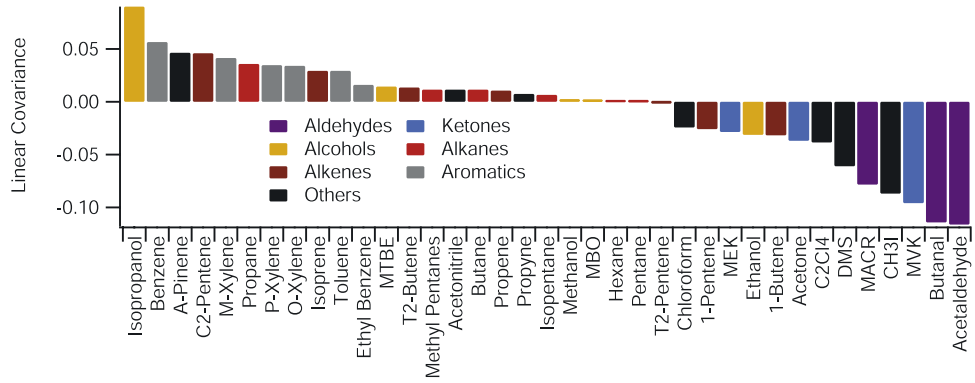

Figure 19. Covariance plot of the *m*/*z* 57 to total organic ratio. This ratio is a measure of the prevalence of long aliphatic chains seen in primary organic aerosol and other less oxidized organic chemicals in the particle phase. The order of the VOCs when compared is virtually reversed compared to the *m*/*z* 44 ratio analysis, showing that the primary organics are associated with fresh emissions.

and organic chemicals. The organic component bore a mass spectral signature that indicated a high degree of chemical oxidation in this fraction. These observations are consistent with the relatively long atmospheric residence times expected. There is also evidence for the presence of very low levels of nitrate and possibly some organic nitrogen compounds, although the exact nature of the latter cannot be rigorously determined at this stage. By using MTBE concentrations as a tracer for local, land-based emissions, a size and chemically resolved mass distribution for ''clean'' MBL air was separated and compared with a locally influenced distribution. It was found that the local influences increased the loadings of ammonium, nitrate and organics. The sulfate was largely unaffected overall, although there were isolated incidents where land-based sulfate sources were observed.

[49] When compared with the PILS-IC instrument, the total mass concentrations of AMS-measured inorganic species, except sea salt, compared favorably. Sea salt concentrations measured by the AMS trended well with and were typically 30% of those from the PILS-IC. The level of oxidation in the organic component varied according to the recent air history and could be linked to the amount of oxidation of the volatile organics observed in the gas phase with a GC-MS-FID, which in turn can be linked to the photochemical history of the air.

[50] A second particle mode of sodium chloride was observed, which was mainly present in the coarse mode. There was also evidence for the presence of sodium nitrate in this mode, implying nitric acid deposition from the gas phase and chloride displacement. The inlet temperature control also provided some very interesting insights into particle behavior with changes in relative humidity and differences in the focusing behavior of solid and liquid particles in the instrument's aerodynamic lens. It appears that as the inlet temperature approaches the ambient dew point, the particles deliquesce and become more spherical, causing the instrument's lens efficiency to increase and the overall sensitivity to approximately double for accumulation mode particles. The quantification of these effects and their physical basis is the subject of ongoing laboratory work.

[51] **Acknowledgments.** This work was funded by the National Oceanographic and Atmospheric Administration (NOAA). During this work, James D. Allan was in receipt of a UK Natural Environment Research Council (NERC) studentship ref. NER/S/A/2000/03653. The UMIST AMS was purchased and maintained through NERC research grant GR3/12499. Many thanks to Eric Williams at the NOAA Aeronomy Laboratory, 325 Broadway, Boulder, CO for the NO_y data and Tim Bates at the NOAA Pacific Marine Environmental Laboratory for the organic and elemental carbon data. The authors gratefully acknowledge the NOAA Air Resources Laboratory for the provision of the HYSPLIT transport and dispersion model (http://www.arl.noaa.gov/ready/hysplit4.html). The coastline data used in the trajectory plots were taken from the National Geophysical Data Center coastline generator website (http://rimmer.ngdc.noaa.gov/coast/getcoast.html). Many thanks to the Humbolt State University Marine Laboratory for the provision of the measurement site and support during the experiment. Additional thanks are given to Robert Prescott at Aerodyne Research Inc. for logistical support.

References

Alfarra, M. R., H. Coe, J. D. Allan, K. N. Bower, P. I. Williams, A. A. Garforth, M. R. Canagaratna, D. R. Worsnop, J. T. Jayne, and J. L. Jimenez (2002), 13B2: Measurements of size resolved organic particulate mass using an on-line aerosol mass spectrometer (AMS): Laboratory validation, analysis tool development and interpretation of field data, paper presented at 21st Annual AAAR Conference, Am. Assoc. for Aerosol Res., Charlotte, N. C.

Alfarra, M. R., et al. (2004), Characterization of urban and rural organic particulate in the lower Fraser valley using two aerodyne aerosol mass spectrometers, *Atmos. Environ.*, in press.

Allan, J. D., J. L. Jimenez, P. I. Williams, M. R. Alfarra, K. N. Bower, J. T. Jayne, H. Coe, and D. R. Worsnop (2003a), Quantitative sampling using an Aerodyne aerosol mass spectrometer: 1. Techniques of data interpretation and error analysis, *J. Geophys. Res.*, *108*(D3), 4090, doi:10.1029/2002JD002358.

Allan, J. D., et al. (2003b), Quantitative sampling using an Aerodyne aerosol mass spectrometer: 2. Measurements of fine particulate chemical composition in two U.K. cities, *J. Geophys. Res.*, *108*(D3), 4091, doi:10.1029/2002JD002359.

Allan, J. D., M. R. Alfarra, K. N. Bower, H. Coe, J. T. Jayne, D. R. Worsnop, P. Aalto, M. Kulmala, and A. Laaksonen (2003c), 1C3: Measurements of fine particle composition during Quest 2 in the Boreal Forest, Finland using an aerodyne aerosol mass spectrometer, paper presented at 22nd Annual AAAR Conference, Am. Assoc. for Aerosol Res., Anaheim, Calif.

Atkinson, R., D. L. Baulch, R. A. Cox, R. F. Hampson, J. A. Kerr, M. J. Rossi, and J. Troe (1997), Evaluated kinetic, photochemical and heterogeneous data for atmospheric chemistry: Supplement V, IUPAC subcommittee on gas kinetic data evaluation for atmospheric chemistry, *J. Phys. Chem. Ref. Data*, *26*(3), 521–1011.

Ayers, G. P., J. P. Ivey, and R. W. Gillett (1991), Coherence between seasonal cycles of dimethyl sulfide, methanesulfonate and sulfate in marine air, *Nature*, *349*(6308), 404–406.

Berg, O. H., E. Swietlicki, and R. Krejci (1998), Hygroscopic growth of aerosol particles in the marine boundary layer over the Pacific and Southern Oceans during the First Aerosol Characterization Experiment (ACE 1), *J. Geophys. Res.*, *103*(D13), 16,535–16,545.

Buzorius, G., A. Zelenyuk, F. Brechtel, and D. Imre (2002), Simultaneous determination of individual ambient particle size, hygroscopicity and composition, *Geophys. Res. Lett.*, *29*(20), 1974, doi:10.1029/2001GL014221.

Canagaratna, M. R., et al. (2003), Chase studies of particulate emissions from in-use New York City vehicles, *Aerosol Sci. Technol.*, in press.

Charlson, R. J., J. E. Lovelock, M. O. Andreae, and S. G. Warren (1987), Oceanic Phytoplankton, Atmospheric Sulfur, Cloud Albedo and Climate, *Nature*, *326*(6114), 655–661.

Coplen, T. B., et al. (2002), Isotope-abundance variations of selected elements: IUPAC technical report, *Pure Appl. Chem.*, *74*(10), 1987–2017.

Drewnick, F., J. J. Schwab, O. Hogrefe, S. Peters, L. Husain, D. Diamond, R. Weber, and K. L. Demerjian (2003), Intercomparison and evaluation of four semi-continuous PM2. 5 sulfate instruments, *Atmos. Environ.*, *37*(24), 3335–3350.

Goldstein, A. H., S. C. Wofsy, and C. M. Spivakovsky (1995), Seasonal-Variations of Nonmethane Hydrocarbons in Rural New England: Constraints on OH Concentrations in Northern Midlatitudes, *J. Geophys. Res.*, *100*(D10), 21,023–21,033.

Jayne, J. T., D. C. Leard, X. F. Zhang, P. Davidovits, K. A. Smith, C. E. Kolb, and D. R. Worsnop (2000), Development of an aerosol mass spectrometer for size and composition analysis of submicron particles, *Aerosol Sci. Technol.*, *33*(1–2), 49–70.

Jimenez, J. L., et al. (2003a), Ambient aerosol sampling using the Aerodyne Aerosol Mass Spectrometer, *J. Geophys. Res.*, *108*(D7), 8425, doi:10.1029/2001JD001213.

Jimenez, J. L., R. Bahreini, D. R. Cocker, H. Zhuang, V. Varutbangkul, R. C. Flagan, J. H. Seinfeld, C. D. O'Dowd, and T. Hoffmann (2003b), New particle formation from photooxidation of diiodomethane (CH2I2), *J. Geophys. Res.*, *108*(D10), 4318, doi:10.1029/2002JD002452.

Jobson, B. T., Z. Wu, H. Niki, and L. A. Barrie (1994), Seasonal trends of isoprene, C2–C5 alkanes and acetylene at a remote boreal site in Canada, *J. Geophys. Res.*, *99*(D1), 1589–1599.

Laturnus, F., K. F. Haselmann, T. Borch, and C. Gron (2002), Terrestrial natural sources of trichloromethane (chloroform, CHCl3): An overview, *Biogeochemistry*, *60*(2), 121–139.

Linstrom, P. J., and W. G. Mallard (2003), NIST Chemistry WebBook, *NIST Standard Reference Database Number 69*, Natl. Inst. of Standards and Technol., Gaithersburg, Md.

Liu, P., P. J. Ziemann, D. B. Kittelson, and P. H. McMurry (1995a), Generating Particle Beams of Controlled Dimensions and Divergence: I. Theory of Particle Motion in Aerodynamic Lenses and Nozzle Expansions, *Aerosol Sci. Technol.*, *22*(3), 293–313.

Liu, P., P. J. Ziemann, D. B. Kittelson, and P. H. McMurry (1995b), Generating Particle Beams of Controlled Dimensions and Divergence: II. Experimental Evaluation of Particle Motion in Aerodynamic Lenses and Nozzle Expansions, *Aerosol Sci. Technol.*, *22*(3), 314–324.

Matthew, B., and A. M. Middlebrook (2003), 4PE7: Percent transmission of ammonium nitrate and ammonium sulfate particles as a function of re-

lative humidity for an aerodyne aerosol mass spectrometer, paper presented at 22nd Annual AAAR Conference, Am. Assoc. for Aerosol Res., Anaheim, Calif.

Millet, D. B., et al. (2004), Volatile organic compound measurements at Trinidad Head, California, during ITCT 2K2: Analysis of sources, atmospheric composition, and aerosol residence times, *J. Geophys. Res.*, *109*, D23S16, doi:10.1029/2003JD004026, in press.

Orsini, D. A., Y. L. Ma, A. Sullivan, B. Sierau, K. Baumann, and R. J. Weber (2003), Refinements to the particle-into-liquid sampler (PILS) for ground and airborne measurements of water soluble aerosol composition, *Atmos. Environ.*, *37*(9-10), 1243–1259.

Press, W. H. (1992), *Numerical Recipes in C: The Art of Scientific Computing*, Cambridge Univ. Press, New York.

Quinn, P. K., D. S. Covert, T. S. Bates, V. N. Kapustin, D. C. Ramseybell, and L. M. Mcinnes (1993), Dimethylsulfide/cloud condensation nuclei/climate system: Relevant size-resolved measurements of the chemical and physical properties of atmospheric aerosol particles, *J. Geophys. Res.*, *98*(D6), 10,411–10,427.

Raes, F., R. Van Dingenen, E. Vignati, J. Wilson, J. P. Putaud, J. H. Seinfeld, and P. Adams (2000), Formation and cycling of aerosols in the global troposphere, *Atmos. Environ.*, *34*(25), 4215–4240.

Semadeni, M., D. W. Stocker, and J. A. Kerr (1995), The temperature dependence of the OH radical reactions with some aromatic compounds under simulated tropospheric conditions, *Int. J. Chem. Kinet.*, *27*(3), 287–304.

Sharma, S., L. A. Barrie, D. Plummer, J. C. McConnell, P. C. Brickell, M. Levasseur, M. Gosselin, and T. S. Bates (1999), Flux estimation of oceanic dimethyl sulfide around North America, *J. Geophys. Res.*, *104*(D17), 21,327–21,342.

Shrestha, R. M., S. C. Bhattacharya, and S. Malla (1996), Energy use and sulphur dioxide emissions in Asia, *J. Environ. Manage.*, *46*(4), 359–372.

Swietlicki, E., et al. (2000), Hygroscopic properties of aerosol particles in the northeastern Atlantic during ACE-2, *Tellus Ser. B*, *52*(2), 201–227.

Topping, D., H. Coe, G. McFiggans, R. Burgess, J. D. Allan, M. R. Alfarra, K. N. Bower, T. W. Choularton, S. Decesari, and M. C. Facchini (2004), Aerosol chemical characteristics from sampling conducted on the island of Jeju, Korea during ACE Asia, *Atmos. Environ.*, *38*(14), 2111–2123.

Wallington, T. J., J. M. Andino, L. M. Skewes, W. O. Siegl, and S. M. Japar (1989), Kinetics of the reaction of OH radicals with a series of ethers under simulated atmospheric conditions at 295 K, *Int. J. Chem. Kinet.*, *21*(11), 993–1001.

Weber, R. J., D. Orsini, Y. Daun, Y. N. Lee, P. J. Klotz, and F. Brechtel (2001), A particle-into-liquid collector for rapid measurement of aerosol bulk chemical composition, *Aerosol Sci. Technol.*, *35*(3), 718–727.

Zhang, X. F., K. A. Smith, D. R. Worsnop, J. Jimenez, J. T. Jayne, and C. E. Kolb (2002), A numerical characterization of particle beam collimation by an aerodynamic lens-nozzle system: I. An individual lens or nozzle, *Aerosol Sci. Technol.*, *36*(5), 617–631.

J. D. Allan, K. N. Bower, and H. Coe, Department of Physics, University of Manchester Institute of Science and Technology, PO Box 88, Manchester, M60 1QD, UK. (james.allan@physics.org)

H. Boudries, M. R. Canagaratna, J. T. Jayne, and D. R. Worsnop, Aerodyne Research Inc., 45 Manning Road, Billerica, MA 01821, USA.

A. H. Goldstein and D. B. Millet, Environmental Science, Policy and Management, University of California at Berkeley, 151 Hilgard Hall, Berkeley, CA 94720, USA.

P. K. Quinn, NOAA Pacific Marine Environmental Laboratory, 7600 Sand Point Way NE, Seattle, WA 98115, USA.

R. J. Weber, School of Earth and Atmospheric Sciences, Georgia Institute of Technology, 311 Ferst Drive, Atlanta, GA 30332, USA.